Use of airborne LiDAR to delineate canopy degradation and encroachment along the Guatemala-Belize border

Authors: Weishampel, John F. , Hightower, Jessica N. , Chase, Arlen F. , and Chase, Diane Z.

Research Article

Use of airborne LiDAR to delineate canopy degradation and encroachment along the Guatemala-Belize border

John F. Weishampel[1,*], Jessica N. Hightower[1], Arlen F. Chase[2], and Diane Z. Chase[2]

Departments of [1]Biology and [2]Anthropology, University of Central Florida, Orlando, FL 32816 USA

*author for correspondence: John.Weishampel@ucf.edu

Abstract

Tropical rainforest clearing and degradation significantly reduces carbon sequestration and increases the rate of biodiversity loss. There has been a concerted international effort to develop remote sensing techniques to monitor broad-scale patterns of forest canopy disturbance. In addition to loss of natural resources, recent deforestation in Mesoamerica threatens historic cultural resources that for centuries lay hidden below the protective canopy. Here, we compare satellite-derived measures of canopy disturbance that occurred over a three decade period since 1980 to those derived from a 2009 airborne LiDAR campaign over the Caracol Archaeological Reserve in western Belize. Scaling up fine-resolution canopy height measures to the 30 m resolution of Landsat Thematic Mapper, we found LiDAR revealed a >58% increase in the extent of canopy disturbance where there was an overlap of the remotely sensed data sources. For the entire archaeological reserve, with the addition of LiDAR, there was a 2.5% increase of degraded canopy than estimated with Landsat alone, indicating that 11.3% of the reserve has been subjected to illegal selective logging and deforestation. Incursions into the reserve from the Guatemala border, represented by LiDAR-detected canopy disturbance, extended 1 km deeper (to 3.5 km) into Belize than were derived with Landsat. Thus, while LiDAR enables a synoptic, never-seen-before, below-canopy view of the Maya city of Caracol, it also reveals the degree of canopy disturbance and potential looting of areas yet to be documented by archaeologists on the ground.

Keywords: Canopy degradation, Deforestation, Edge detection, Landsat, LiDAR, Maya archaeology, REDD+, Selective logging, Wombling

Resumen

La tala y el deterioro de los bosques húmedos tropicales reducen significativamente la habilidad de este ecosistema para capturar carbono, y aumentan la tasa de pérdida de biodiversidad. Por lo tanto, existe un esfuerzo internacional para desarrollar técnicas de sensores remotos con el fin de monitorear los patrones a gran escala de las perturbaciones en el dosel del bosque. Adicional a la perdida de recursos naturales, la deforestación reciente en Mesoamérica amenaza los recursos históricos culturales que por siglos han permanecido escondidos bajo la protección del dosel. En este proyecto comparamos algunas medidas de perturbación del dosel derivadas de imágenes satelitales durante un periodo de tres décadas a partir de 1980, con aquellas derivadas de una campaña de vuelos con LiDAR llevada a cabo en 2009 sobre la Reserva Arqueológica Caracol en el oeste de Belice. Ampliando las medidas de altura de dosel de resolución fina a la resolución de 30 m del Landsat Thematic Mapper, encontramos que LiDAR reveló un aumento de más de 58% en la extensión de perturbaciones del dosel para aquellas áreas en donde se tenían datos de ambas fuentes de sensores remotos. Para la totalidad de la reserva arqueológica, con la adición de LiDAR hubo un aumento de 2.5% del área perturbada del dosel sobre la estimada utilizando únicamente Landsat, indicando que 11.3% de la reserva ha estado sujeta a tala selectiva ilegal y deforestación. Las incursiones a la reserva desde la frontera con Guatemala, reflejadas por las perturbaciones del dosel detectadas con LiDAR, se adentran 1 km más en Belice (hasta 3.5 km) que aquellas derivadas con Landsat. Por lo tanto, además de proporcionar una mirada sinóptica, nunca antes vista de la ciudad Maya de Caracol bajo del dosel, LiDAR también revela el grado de perturbación del dosel y el saqueo potencial de terrenos que aún no han sido documentados por arqueólogos.

Palabras clave: degradación del dosel, deforestación, detección de bordes, Landsat, LiDAR, arqueología Maya, REDD+, tala selectiva, "wombling".

Introduction

Not since the heyday of the Maya civilization (≈1200 years BP) has Mesoamerica experienced the level of deforestation that is presently occurring [1]. In Belize, this has been documented over the last few decades in a series of optical satellite remote sensing studies (e.g., [2-4]) that analyzed imagery from the Landsat Multispectral Scanner (MSS) and Thematic Mapper (TM) sensors. Though exhibiting a decline in forest cover of >13% since 1980, Belize remains proportionately (≈60%) the most forested country in Central America [3]. These forested areas function as important components of the Mesoamerican Biological Corridor [5], which is being continually threatened by changes in human land use patterns within and beyond Belize [6-7].

In addition to domestic resource use, Belize forests are also subject to extensive cross-border incursions that result in illegal forest clearing for timber harvesting, milpa farming, selective logging (Fig. 1), and animal and Xaté (threatened palm species of the genus *Chamaedorea*) poaching [8-9]. These actions relate to increased environmental pressures from neighboring Guatemala, whose population has doubled since 1985, and in part, to a more than 150-year-old border dispute that pre-dates the establishment of an independent Belize in 1981.

Expectations are high for LiDAR (Light Detection And Ranging), with its ability to capture detailed forest structural information (e.g., [10-14]) and quantify biomass levels (e.g., [15-16]) to contribute to the REDD+ (Reducing Emissions from Deforestation and forest Degradation and enhancing forest carbon stocks) monitoring of tropical carbon reserves [17-20]. The large-footprint (≈64 m diameter) Geoscience Laser Altimeter System (GLAS) onboard the Ice, Cloud, and land Elevation Satellite (ICESat) has been recently used to establish a global baseline of carbon stocks [21]. However, high-resolution, small-footprint (≈1 m horizontal resolution) LiDAR coverage over broad areas is expensive to acquire in comparison to optical imagery (e.g., aerial photography and satellite imagery [18, 22]), and hence, up to this point, has not been used to monitor patterns of regional deforestation and forest degradation [20]).

Though a methodology to use small-footprint airborne LiDAR in concert with optical imagery for fine resolution REDD+ assessment has been developed by Asner [19], in this study we directly compare optical satellite sensor (i.e., Landsat [3]), and airborne LiDAR-derived estimates and patterns of forest deforestation/degradation in the Caracol Archaeological Reserve located along the Belize-Guatemala border.

Fig. 1. Scene of small cleared area with recently cut log remains and open canopy located to the southwest of the Caracol epicenter (photocredit: J. Hightower).

Methods

Caracol Study Area

The Caracol Archaeological Reserve (CAR) is a 10,340 ha restricted area (Fig. 2) designated in 1995 by the Ancient Monuments and Antiquities Act authorized by the Government of Belize to protect the Maya site of Caracol, the largest archaeological ruin in Belize. The reserve, located on the western border next to Guatemala on the Vaca Plateau in the Cayo District, is adjacent to the Chiquibul National Park (CNP), Belize's largest national park, in close proximity to the Chiquibul Forest Reserve (CFR). These three forested areas consist largely of lowland to submontane broad-leaved moist to wet forests [23]. They are part of the largest remaining contiguous block of neo-tropical forest north of the Amazon.

These forests are subject to periodic hurricane disturbance; Hurricane Hattie in 1961 downed up to 90% of canopy trees in some areas of Belize, even though it left other sheltered areas intact [24]. This disturbance was followed by fires [25] in some of the drier areas. Hurricane Greta in 1978 was the last significant hurricane in the general Caracol vicinity [26]. Historically, these forests have been subjected to a variety of management practices, such as chicle extraction, salvage logging after windthrow, and selective logging of valuable timber species such as mahogany (*Swietenia macrophylla* King) and Spanish cedar (*Cedrella odorata* L.); however, since 1994 only limited sustainable practices have been permitted in CFR [27]. Other than work efforts related to sanctioned archaeological excavation, no harvesting is permitted in CAR. The average canopy height around the Caracol epicenter (i.e., an area with a high concentration of large monumental Maya architecture and the center of the site from which ancient causeways radiate) ranges from 20 to 25 m with a few emergent trees reaching up to 35 m; the vertical structure is homogenous with no distinct layering [28].

Remotely Sensed Data Acquisition and Processing

As part of a NASA Space Archaeology [29] project described in Weishampel et al. [30], LiDAR data (Fig. 3) were collected by the National Center for Airborne Laser Mapping (NCALM) using an Optech GEMINI Airborne Laser Terrain Mapper (ALTM) from a ≈200 km^2 area that was believed to represent the extent of the Maya city of Caracol. In late April 2009, the sensor flew onboard a twin-engine Cessna Skymaster at an average altitude of 800 m above ground level. Coverage consisted of 60 east-west and 62 north-south flight lines separated by 260 m [31]. With a sensor scan frequency of 40 Hz and a scan angle of ±21°, the swath width was ≈520 m, providing 200% overlap. The LiDAR coverage included most of CAR except a ≈315 ha triangular sliver in the southwest corner of the reserve adjacent to the Guatemala border that was not part of the request to NCALM, and an irregular ≈60 ha area in the northwest corner where there was cloud cover during the flights (Fig. 2).
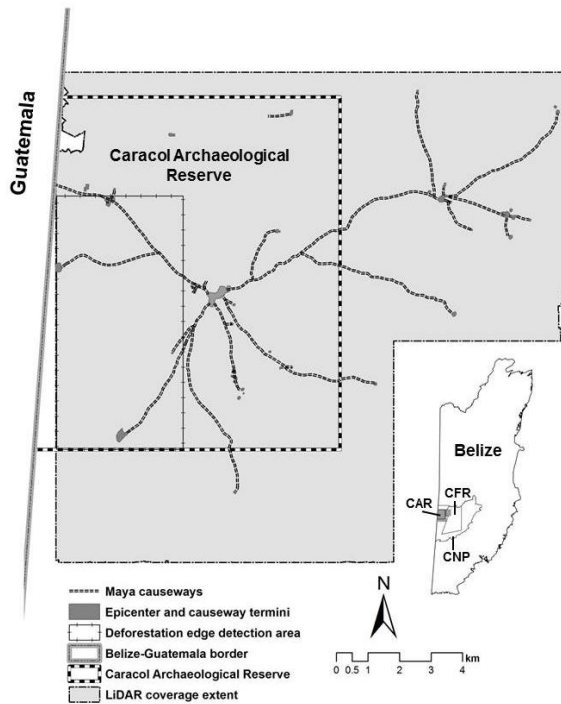

Fig. 2. Focus areas analyzed in the Caracol Archaeological Reserve (CAR) which is located next to the Chiquibil National Park (CNP) and Chiquibil Forest Reserve (CFR) and adjacent to the Guatemalan border as shown in the Belize inset.

On average, there were 20 measurement points per square meter, of which ≈1.35 points m^{-2} passed through gaps in the canopy and reached the ground. These were interpolated by NCALM to derive a 1-m resolution digital elevation model (DEM) with a root mean square (RMS) error between 0.02 and 0.03 m. This DEM was instrumental for the subsequent archaeological [31-33] and geomorphological [34] studies. NCALM researchers also created a 1-m resolution canopy surface model (CSM) using interpolation and surface generating algorithms for all the highest non-ground points. The difference between the CSM and DEM was used to provide a model of canopy height (CHM). Though the 20 points·m^{-2} density is considerably higher than most commercial LiDAR data acquisitions, we reduced the data by 75% (which is on par with typical acquisitions) and were still able to "see" most ground features suggesting that 4 points·m^{-2} density would be adequate for our canopy analysis.

A. Laser fires 1000s of pulses per second.
- Photons reflect off target and return to receiver.
- Based on speed of light, distance from sensor to the target is calculated.
B. GPS records aircraft latitude, longitude, and altitude.
C. Inertial navigation unit records aircraft's orientation (roll, pitch, and yaw).
D. On-board computer converts locations of target surfaces into 3-dimensional (x,y,z) data called point clouds.
E. Difference between 1st posting (canopy top height) and last return (ground) yields the canopy height model.
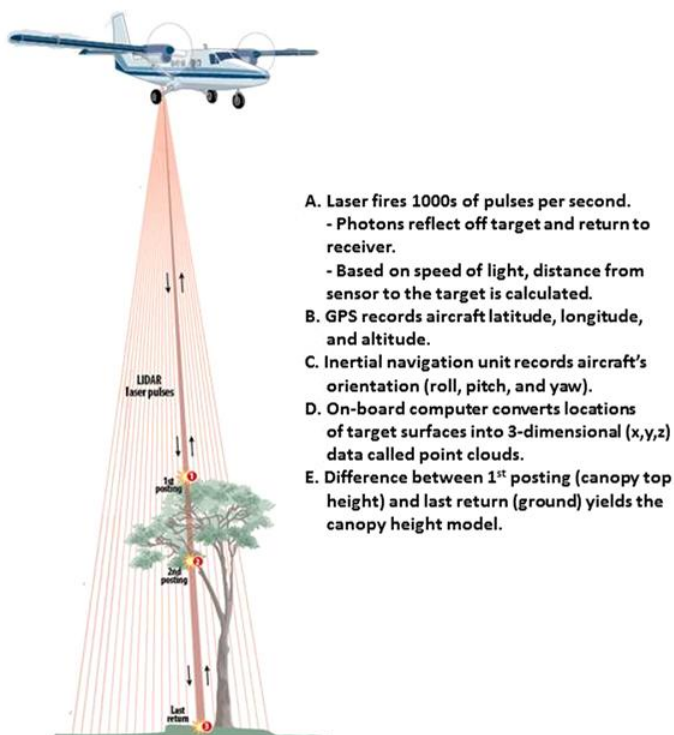
Fig. 3. Diagram depicting how the LiDAR system records the location of canopy and ground surfaces and how the canopy height model (CHM) is derived (adapted from graphics developed by S. Floyd).

Two IKONOS images acquired just prior to the NCALM flights (12 March 2009 and 3 April 2009) that covered most of the Caracol Archaeological Reserve were purchased to allow for visual comparison with the CHM in areas that had been deforested since 1980 and very recently cleared areas (Fig. 4). Based on this assessment, canopy heights ≤7.5 m were designated as cleared or disturbed which is considerably higher than the 2 m gap definition of Brokaw [35] but corresponded well with the Landsat-derived deforested areas [3] and the more extensively disturbed areas visible in the IKONOS images. The 7.5 m value also corresponded to the average height of the non-forest category from Cherrington et al. [3] which represented areas that did not have forest cover between 1980 and 2010. The density of these disturbed areas (or canopy gaps) in the CHM was calculated within 30 x 30 m pixel areas for comparative purposes with the Landsat TM deforestation study [3], using ArcGIS 9.3 software. Thus, each pixel value was a measure of the density of gaps (i. e., 1 m^2 areas with height values <7.5 m) in the 900 m^2 area.

Comparison of LiDAR- and Landsat-Derived Deforestation
The somewhat coincident Landsat deforestation study [3] that included TM scenes from January and February of 2010 and the LiDAR collection from late April 2009 allowed for a comparison of deforestation patterns assessed by the two sensor systems. The Landsat study mapped five periods of deforestation over three decades. LiDAR-derived canopy heights for these five deforestation periods were measured to assess canopy regrowth or recovery. For the area of overlap in CAR within 5 km of the Guatemala boarder, there was: 4639.9 ha of intact forest; 15.6 ha of non-forest; 2.7 ha of area that was cleared from 1980 to 1989; 23.9 ha that was cleared from 1989 to 1994; 175.4 ha that was cleared from 1994 to 2000; 150.12 ha that was cleared from 2000 to 2004; and 202.3 that was cleared from 2004 to 2010. In addition, the levels of deforestation/disturbance, as a function of distance from the Guatemala border, and the overall level of disturbance in CAR, as determined by the two techniques, were evaluated.

To identify locations of deforestation/canopy disturbance recorded with LiDAR and to assess if there was a gradient of disturbance from the Guatemala border, we employed continuous or lattice wombling [36] to delineate edges in the 30 m resolution gap density map. This technique assessed the magnitude (m) and direction (x and y) of contrast at each intersection (common corner) of four pixels (A, B, C, D) of value Z_i that form a square where:

$$m = \sqrt{\left[\frac{\partial f(x,y)}{\partial x}\right]^2 + \left[\frac{\partial f(x,y)}{\partial y}\right]^2} \qquad \textbf{Equation 1}$$

and

$$f(x,y) = Z_A(1-x)(1-y) + Z_B x(1-y) + Z_C xy + Z_D(1-x)y \qquad \textbf{Equation 2}$$

We applied this method across an 8 x 4 km rectangular area with contiguous LiDAR coverage in the western half of CAR (Fig. 3) using the PASSaGE 2 [37] software package. We located elements (corner points) whose magnitudes were in the upper 10% of all intersections and overlaid these point data on the Landsat-derived deforestation maps for a visual comparison of canopy disturbance patterns.
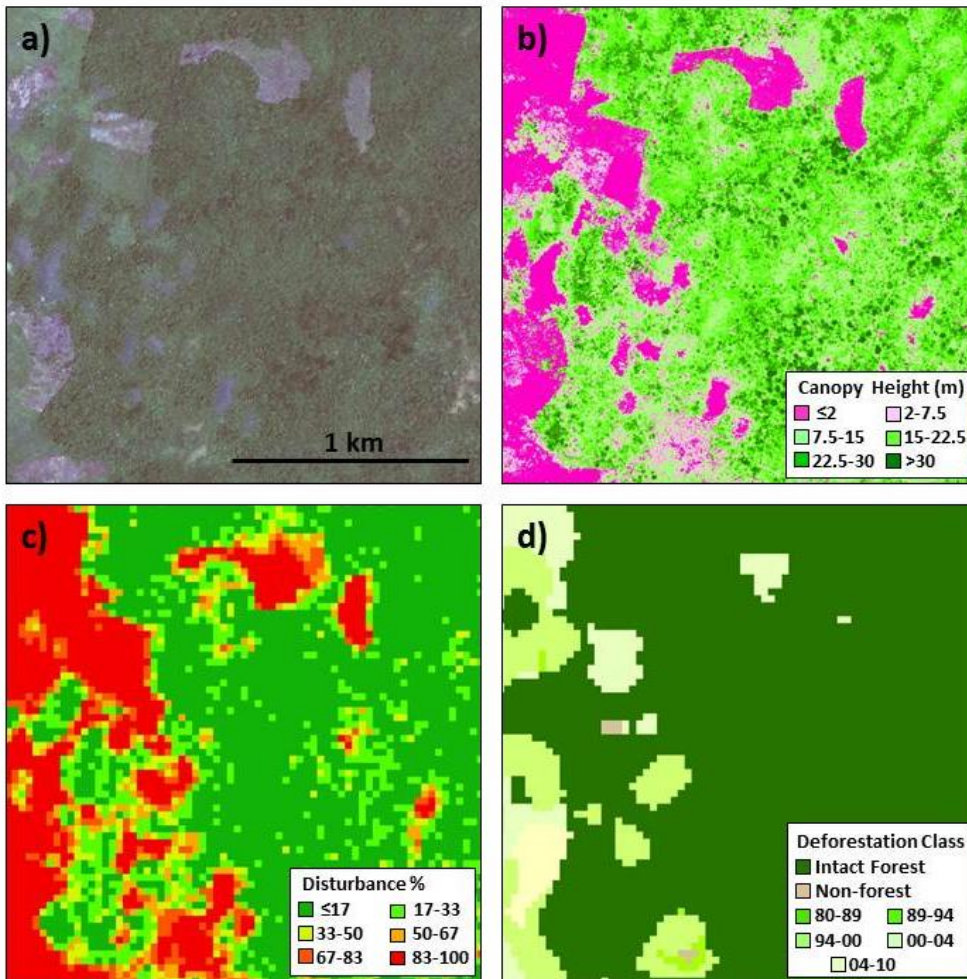

Fig. 4. Four square kilometer area in the southwestern corner of CAR ≈500 m away from the Guatemala border represented by: a) 3 April 2009 IKONOS image; b) CHM derived from LiDAR flown in late April 2009; c) Density map of canopy heights ≤7.5 m rescaled to 30 m to match the Landsat resolution; d) Landsat-derived deforestation map showing the different periods of clearing into late February 2010 (adapted from Cherrington et al. [3]).

Results and Discussion

In CAR most of the deforestation over the last 30 years occurred during the last decade (2000-2010). There was an obvious difference between the LiDAR-derived canopy height measures from intact and deforested areas regardless of the time since deforestation (Fig. 5). The average canopy height of the intact forests was 16.9 m compared to an average of 2.1 m for all five periods of deforestation. This suggests that most of the deforested areas continued to be used for agriculture or pastureland, and hence forests were not permitted to regenerate. The non-forest category had a 7.1 m tall canopy which may represent: 1) new growth by early successional plants, 2) registration error, or 3) result from the relatively coarse Landsat TM pixel 30-m resolution compared to the 1-m LiDAR CHM resolution [38] which was aggregated to 30 m. Because this approach to measure canopy height records the highest point within each 1 m^2 area, it is expected that the height estimate would be lower than Brokaw's [28] measure of ≈20 m which focuses on the height of the top of the canopy dominant trees, but ignores lower heights of canopy envelope.

Deforestation from the Guatemala border, as estimated by the Landsat study, extended about 2.5 km into CAR with nearly 50% of the CAR canopy cleared 1 km into Belize (Fig. 6). The estimate of canopy disturbance from the Guatemala border increased to about 3.5 km based on the LiDAR data with 50% of the canopy showing signs of disturbance 1.4 km into Belize (Fig. 7). As expected, canopy height was inversely related to the presence of canopy gaps. Beyond 3.5 km eastward from the border, the canopy height measures and the proportion of canopy gaps leveled off. This discrepancy between the Landsat- and LiDAR-derived deforested/disturbed canopy patterns was also apparent in wombling edge detection analysis (Fig. 8). The edges between forest and non-forest or disturbed canopy projected further into Belize in the LiDAR data. Substantial canopy disturbance was found adjacent to the Landsat-derived deforestation edges. Several pockets of forest clearing several kilometers from the Guatemalan border that were not identified in the 30-m resolution Landsat product were manifest in the scaled-up 30-m resolution LiDAR product. Some of these, however, were visible in the IKONOS image, as depicted in Figure 3. This may reflect several possibilities: 1) cloud cover during the Landsat scene acquisition may have prevented the capture of the recent more extensive deforestation events, and/or 2) the coarser Landsat resolution may preclude identifying finer scale logging events. Though at the broader extent (e.g., Fig. 4), the LiDAR and IKONOS data showed similar deforestation/degradation patterns, when zooming in, the smaller LiDAR-detected gap patterns were not visible in the IKONOS scene.
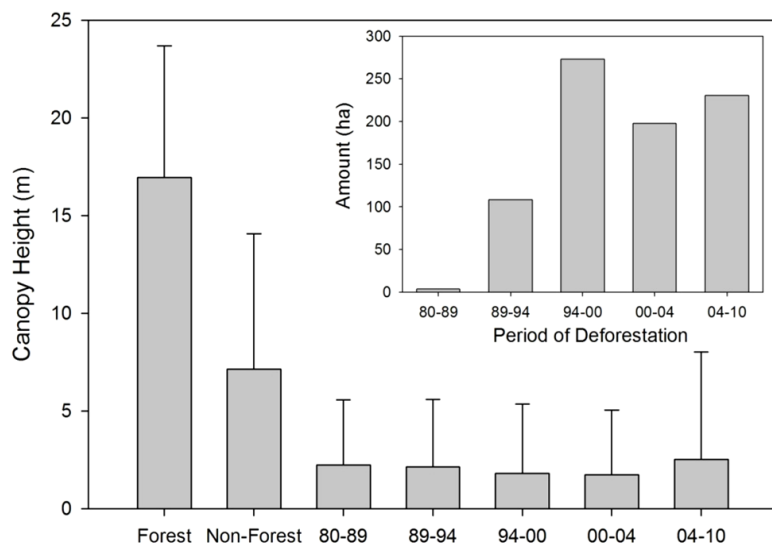

Fig. 5. Relationships of Landsat-derived land cover classes and LiDAR-derived canopy height measures in CAR. Extensions represent standard deviation of height measures for the 1 m^2 pixels from the CHM for each class. The inset shows the extent of deforestation in CAR for five time periods since 1980 as estimated with Landsat by Cherrington et al. [3].

In areas of overlapping coverage, using the cutoff of ≥50% density of canopy heights ≤7.5 m to represent a disturbed canopy, LiDAR detected 58.3% more non-intact canopy than the Landsat study at CAR: this amounted to an overall 40% higher estimate of disturbance at CAR (Appendix 1). The extent of disturbed canopies based on combining estimates from Landsat for the area not covered by LiDAR plus the estimates from LiDAR amounts to over 11% of CAR. This is a conservative estimate, as additional clearing most likely occurred between the LiDAR flights (May 2009) and the last Landsat TM scene (February 2010) which was not detected in the satellite image. This demonstrates the application of airborne LiDAR as a sensitive tool to monitor canopy integrity in areas affected by selective logging or patchy forest clearing. Such selective logging, though relatively low impact in terms of canopy disturbance and soil compaction compared to more intensive clearing, may not be sustainable [39]. It should additionally be noted that, because of the multiple laser returns gained through LiDAR, it also may be possible to determine whether the undergrowth has been cleared beneath the canopy, a practice usually undertaken to plant illegal substances like marijuana and avoid direct aerial detection.
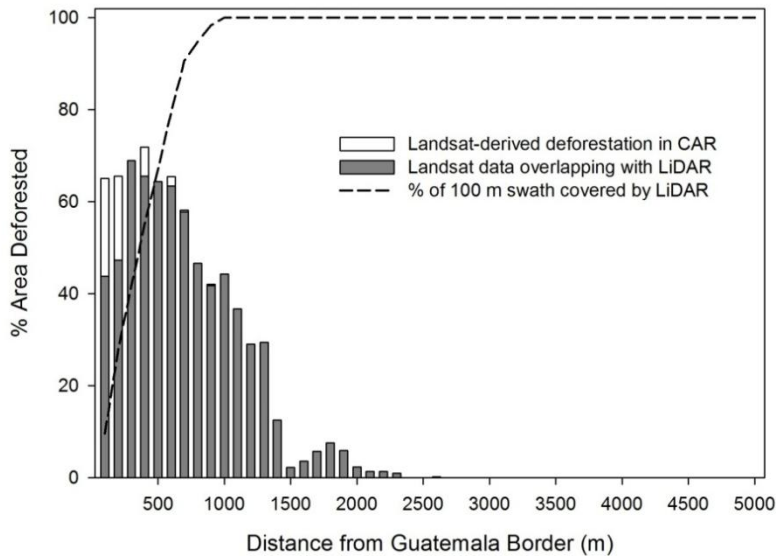

Fig. 6. Percent CAR area deforested in 100 m wide swaths from the Guatemala border based on Landsat estimates of Cherrington et al. [3]. The shaded bars depict the percent area deforested in regions of the swaths that were covered by LiDAR whose relative coverage per swath is shown by the dashed line.
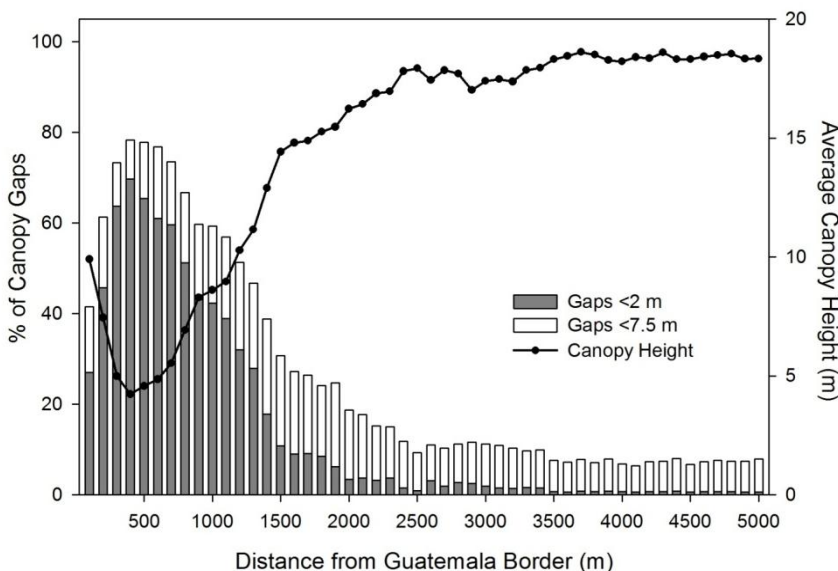

Fig. 7. Percent of disturbed canopy or gaps (designated by heights ≤2 m and ≤7.5 m) and average canopy height in the 100 m swaths located in CAR from the Guatemala border as determined by LiDAR.

Implications for Conservation

Addressing the problem of deforestation/forest degradation is critical as, during the 2009-11 archaeological field seasons (January-March), the sounds of chainsaws were heard almost daily by researchers working near the epicenter which is located ≈6 km from the border. Researchers repeatedly stumbled upon small cleared areas, some with planks remaining and evidence of horse paths that were used to transport the lumber (like that shown in Fig. 1). Unfortunately, as we are learning more about the archaeological remains at Caracol with LiDAR, this same technology is also detailing extensive modern deforestation and looting along the Guatemala-Belize border that is encroaching several kilometers into the archaeological reserve and threatening the preservation of Belize's cultural and natural heritage. Though expensive compared to more traditional optical sensors, the airborne LiDAR was able to detail fine-scale canopy disturbances associated with selective harvesting of commercially important tree species and the clearing of small patches. The ability to detect these more subtle patterns of canopy degradation with LiDAR may serve as an important sampling technique when attempting to scale-up local biodiversity and/or carbon assessments to broader regions. The use of LiDAR to derive a metric of forest canopy degradation represents one tool available to quantify forest degradation that can be measured in a variety of ways [40].
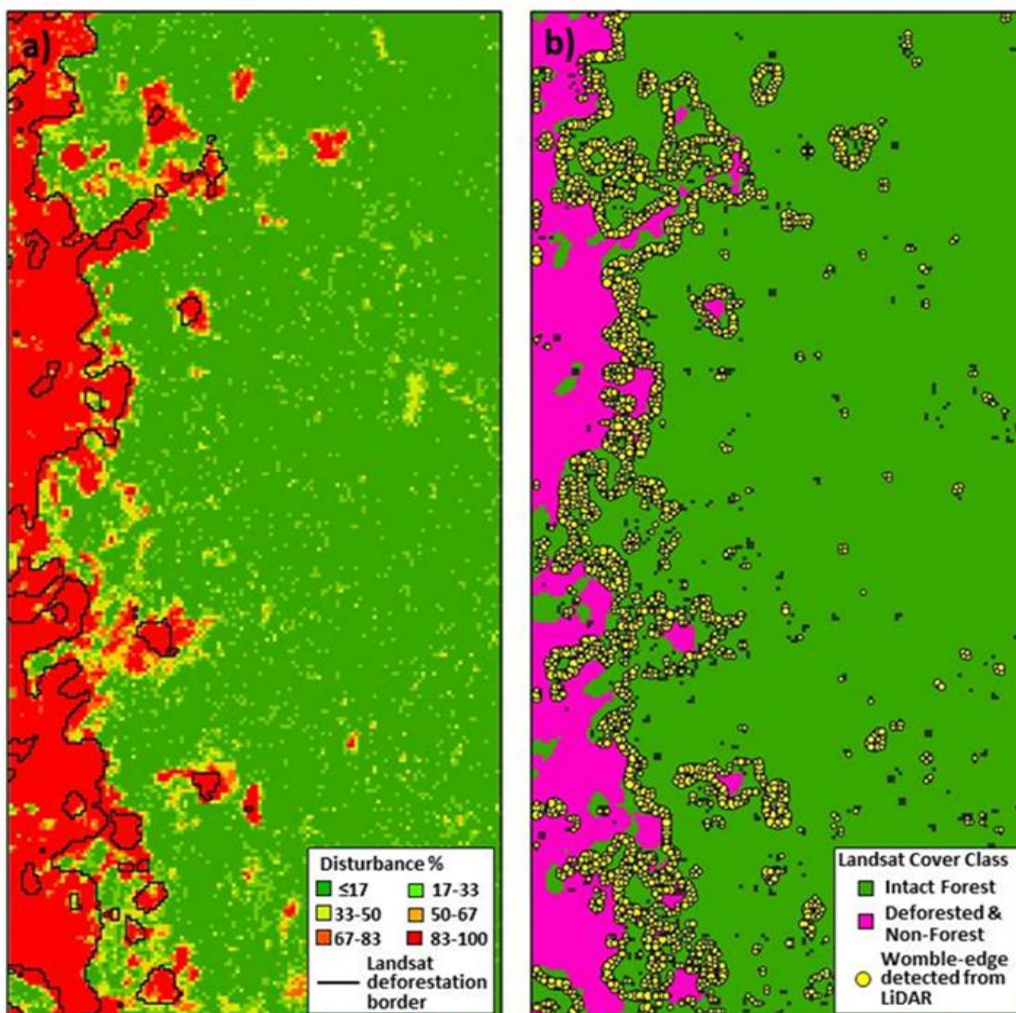

Fig. 8. a) Density of disturbed canopy (i.e., heights ≤ 7.5 m) in 4 x 8 km area in the southwest corner of the LiDAR coverage in CAR. The black outline corresponds to the extent of deforestation from 1980 to 2010 as determined by an analysis of Landsat imagery [3]. b) Corresponding Landsat-derived deforested and intact forest areas overlaid with womble detected edges (yellow circles) from the LiDAR-derived disturbed canopy density map. Circle size corresponds to the relative strength of the edge contrast as calculated by wombling.

Acknowledgements

References

[1] Oglesby R. J., Sever, T. L., Saturno, W. , Erickson III, D. J. and Srikishen, J. 2010. Collapse of the Maya: Could deforestation have contributed? *Journal of Geophysical Research* 115: D12106.

[2] Emch, M., Quinn, J. W., Peterson, M. and Alexander, M. 2005. Forest cover change in the Toledo District, Belize from 1975 to 1999: a Remote sensing approach. *The Professional Geographer* 57: 256-267.

[3] Cherrington, E.A., Ek, E. , Cho, P., Howell, B. F. , Hernandez, B. R., Anderson, E. R., Florez, A. I., Garcia, B. C., Sempris, E. and Irwin, D. E. 2010. *Forest cover and deforestation in Belize: 1980-2010.* SERVIR, Cathalac.

[4] Meerman, J., Epting, J., Steininger, M. and Hewson, J. 2010. *Forest cover and change in Belize circa 1990-2000-2005*. Belize Tropical Forest Studies.

[5] DeClerck, F. A. J., Chazdon, R., Holl, K. D., Milder, J. C., Finegan, B., Martinez-Salinas, A., Imbach, P., Canet, L. and Ramos, Z. 2010. Biodiversity conservation in human-modified landscapes of Mesoamerica: Past, present, and future. *Biological Conservation* 143: 2301-2313.

[6] Vester, H. F. M., Lawrence, D. , Eastman, J. R., Turner, B. L., Calme, S., Dickson, R., Pozo, C. and Sangermano, F. 2007. Land change in the southern Yucatan and Calakmul Biosphere Reserve: Effects on habitat and biodiversity. *Ecological Applications* 17: 989-1003.

[7] Díaz-Gallegos, J. R., Mas, J. F. and Montes, A. V. 2008. Monitoreo de los patrones de deforestación en el Corridor Biológico Mesoamericano, México. *Interciencia* 33: 882-890.

[8] Young, C. A. 2008. Belize's ecosystems: threats and challenges to conservation in Belize*. Tropical Conservation Science* 1: 18-33.

[9] Perez, A., Chin-Ta, C. and Afero, F. 2009. Belize-Guatemala territorial dispute and its implications for conservation. *Tropical Conservation Science* 2: 11-24.

[10] Weishampel, J. F., Blair, J. B., Dubayah, R., Clark, D. B., and Knox, R. G. 2000. Canopy topography of an old-growth tropical rainforest landscape. *Selbyana* 21: 79-87.

[11] Weishampel, J. F., Blair, J. B., Knox, R. G., Dubayah, R. and Clark, D. B. 2000. Volumetric lidar return patterns from an old-growth tropical rainforest canopy. *International Journal of Remote Sensing* 21: 409-415.

[12] Drake, J. B., Dubayah, R. O., Clark, D. B., Knox, R. G., Blair, J. B., Hofton, M. A., Chazdon, R. L., Weishampel, J. F. and Prince, S. 2002. Estimation of tropical forest structural characteristics using large-footprint lidar. *Remote Sensing of Environment* 79: 305-319.

[13] Koukoulas, S. and Blackburn, G. A. 2004. Quantifying the spatial properties of forest canopy gaps using LiDAR imagery and GIS*. International Journal of Remote Sensing* 25: 3049-3071.

[14] Kellner, J. R., Clark, D. B. and Hubbell, S. P. 2009. Pervasive canopy dynamics produce short-term stability in a tropical rain forest landscape. *Ecology Letters* 12: 155-164.

[15] Drake, J. B., Dubayah, R. O., Knox, R. G., Clark, D. B. and Blair, J. B. 2002. Sensitivity of large-footprint lidar to canopy structure and biomass in a neotropical rainforest. *Remote Sensing of Environment* 81: 378-392.

[16] Clark, M. L., Roberts, D. A., Ewel, J. J. and Clark, D. B. 2011. Estimation of tropical rain forest aboveground biomass with small-footprint lidar and hyperspectral sensors. *Remote Sensing of Environment* 115: 2931-2942.

[17] Angelson, A. 2009. *Realising REDD+ : National Strategy and Policy Options*. Bogor Indonesia: Center for International Forestry Research.

[18] Gibbs, H. K., Brown, S., Niles, J. O. and Foley, J. A. 2007. Monitoring and estimating tropical forest carbon stocks: making REDD a reality. *Environmental Research Letters* 2: 045023.

[19] Asner, G. P. 2009. Tropical forest carbon assessment: integrating satellite and airborne mapping approaches. *Environmental Research Letters* 4: 034009

[20] Koch, B. 2010. Status and future of laser scanning, synthetic aperture radar and hyperspectral remote sensing data for forest biomass assessment. *ISPRS Journal of Photogrammetry and Remote Sensing* 65: 581-590.

[21] Saatchi, S. S., Harris, N. L., Brown, S., Lefsky, M., Mitchard, E. T. A., Salas, W., Zutta, B. R., Buermann, W., Lewis, S. L., Hagen, S., Petrova, S., White, L., Silman, M. and Morel, A. 2011. Benchmark map of forest carbon stocks in tropical regions across three continents. *Proceedings of the National Academy of Sciences* 108: 9899-9904.

[22] Pascual, C., Garcia-Abril, A., Cohen, W. and Martin-Fernandez, S. 2010. Relationship between LiDAR derived forest canopy height and Landsat images. *International Journal of Remote Sensing* 31: 1261-1280.

[23] Meerman, J. 2006. *Belize Ecosystems Map version 2004*. Biodiversity and Environmental Resource Data System of Belize, http://www.biodiversity.bz/.

[24] Lewis, O. T. 2001. Effect of experimental selective logging on tropical butterflies. *Conservation Biology* 15: 389-400.

[25] Wolffsohn, A. 1967. Post-hurricane forest fires in British Honduras. *Commonwealth Forestry Review* 46: 233-238.

[26] Friesner, J. 1993. *Hurricanes and the Forests of Belize*. Forest Department. Ministry of Natural Resources and the Environment. Belmopan City, Belize. 20 pp.

[27] CMM. 2011. Chiquibul-Maya Mountain Program. www.mayamountains.org.

[28] Brokaw, N. V. L. 1992. *Vegetation and Tree Flora in the Central Area of the Caracol Archaeological Reserve, Belize*. Manomet Obervatory for Conservation Sciences, Manomet, Massachusetts.

[29] Giardino, M. J. 2011. A history of NASA remote sensing contributions to archaeology. *Journal of Archaeological Science* 38: 2003-2009.

[30] Weishampel, J. F., Chase, A. F., Chase, D. Z., Drake, J. B., Shrestha, R. L., Slatton, K., Awe, J. J., Hightower, J. and Angelo, J. 2010. Remote Sensing of Ancient Maya Land Use Features at Caracol, Belize related to Tropical Rainforest Structure. In *Space, Time, Place: Third International Conference on Remote Sensing in Archaeology*, Campana, S., Forte, M. and Liuzza, C. (Eds.), pp. 45-52. British Archaeological Reports S2118, Archaeopress, Oxford, England.

[31] Chase, A. F., Chase, D. Z. and Weishampel, J. F. 2010. Lasers in the Jungle: Airborne sensors reveal a vast Maya landscape. *Archaeology.* 63: 29-31.

[32] Chase, A. F., Chase, D. Z., Weishampel, J. F., Drake, J. B., Shrestha, R. L., Slatton, K. L., Awe, J. J. and Carter, W. E. 2011. Airborne LiDAR, archaeology, and the ancient Maya landscape at Caracol, Belize. *Journal of Archaeological Science.* 38: 387-398

[33] Chase, D. Z., Chase, A. F., Awe, J. J., Walker, J. H. and Weishampel, J. F. 2011. Airborne LiDAR at Caracol, Belize and the interpretation of ancient Maya society and landscapes. *Research Reports in Belizean Archaeology* 8: 61-73.

[34] Weishampel, J. F., Hightower, J. N., Chase, A. F., Chase, D. Z. and Patrick, R. A. Detection and morphologic analysis of potential below-canopy cave openings in the karst landscape around the Maya polity of Caracol using airborne LiDAR. *Journal of Cave and Karst Studies*. In press.

[35] Brokaw, N. V. L. 1982. The definition of treefall gap and its effect on measures of forest dynamics. *Biotropica* 14: 158-160.

[36] Fortin, M.-J. 1994. Edge detection algorithms for two-dimensional ecological data. *Ecology* 75: 956-965.

[37] Rosenberg, M. S. and Anderson, C. D. 2011. PASSaGE: Pattern Analysis, Spatial Statistics and Geographic Exegesis. Version 2. *Methods in Ecology & Evolution* 2: 229-232.

[38] Weishampel, J. F., Ranson, K. J. and Harding, D. 1996. Remote sensing of forest canopies. *Selbyana* 7: 6-14.

[39] Whitman, A. A., Brokaw, N. V. L. and Hagan, J. M. 1997. Forest damage caused by selection logging of mahogany (*Swietenia macrophylla*) in northern Belize. *Forest Ecology and Management* 92: 87-96.

[40] Joseph, S., Murthy, M. S. R. and Thomas, A. P. 2011. The progress of remote sensing technology in identifying tropical forest degradation: a synthesis of the present knowledge and future perspectives. *Environmental Earth Sciences* 64: 731-741.

Appendix 1. Extent of canopy disturbance and non-forest using 30 m resolution remotely sensed data in CAR west of the epicenter.

	Area (ha)	% of the entire CAR
a) Landsat-derived (1980-2010)	831.33	8.04
b) Landsat-derived (1980-2010) in LiDAR overlap area	570.96	5.52
c) LiDAR-derived (2009) based on 30 m pixels with ≥50% density of ≤7.5 m canopy	903.78	8.74
Total (a+c-b)	1164.15	11.26